33rd Annual International Conference of the IEEE EMBS
Boston, Massachusetts USA, August 30 - September 3, 2011

Microdosimetry applied to nanosecond pulsed electric fields: a comparison on a single cell between real and ideal waveforms

Caterina Merla, *Member, IEEE*, Alessandra Paffi, Francesca Apollonio, *Member, IEEE*, Philippe Leveque, *Member, IEEE*, Micaela Liberti, *Member, IEEE*

***Abstract*— A microdosimetric analysis using ideal and real pulses was carried out in this paper. To perform this goal, authors employed an algorithm developed recently for nsPEF based on Laplace's equation and able to take into account cell compartment dispersivity. A comparison between biphasic real and ideal waveforms was carried out. The ideal pulse induced the highest pore density efficiency, hence evidencing that a device optimization to avoid waveform degradation and losses has a fundamental impact on the performances of the delivered pulses at the single cell level.**

I. Introduction

During the last ten years, a number of biological effects at the cellular and sub-cellular level due to the exposure of cells and tissues to nanosecond pulsed electric fields (nsPEFs) have been evidenced, as exhaustively reported in a recent review [1].

nsPEFs are characterized by an extremely short duration in the nanosecond range and a megavolt per meter amplitude. The reported effects for signals of a few nanoseconds were mainly dependent on pulse duration allowing targeting of both the plasmic membrane and the intracellular organelles [2], [3].

All such proven effects seem to be mediated by nsPEF induced molecular rearrangement of cell membranes with formation of nanometer-sized pores [2]. This phenomenon appears to modify also intracellular functions as the ones related to the calcium pathway [3], or the appearance of cell apoptotic markers [4], as well as the gene expression modulation [5]. Therefore the possibility to exploit such effects for medical applications (e.g. cancer, neurodegenerative diseases) is, at present, the most exiting and promising use of the electromagnetic (EM) fields in medicine.

Manuscript received April 15, 2011.

C. Merla is with the Italian Inter-University Centre for Study of Electromagnetic Fields and Bio-systems (ICEmB) at ENEA, Casaccia Research Centre, Rome, 00123, Italy (e-mail: caterina.merla@ enea.it).

A. Paffi, F. Apollonio, M. Liberti are with ICEmB at "Sapienza" University of Rome, Rome, 00184, Italy. (e-mail: paffi@die.uniroma1.it, apollonio@die.uniroma1.it, liberti@die.uniroma1.it).

P. Leveque is with the Xlim Research Institut, CNRS-University of Limoges, Limoges, 87060 cedex, France. (e-mail: plilippe.leveque@xlim.fr).

In this context, microdosimetric analysis aiming at the transmembrane potential (TMP) determination and membrane pore density calculation may provide a useful tool supporting biological investigation both *in vitro* and *in vivo*, to highlight the interaction mechanisms at the basis of a rigorous and effective control of medical treatments.

Recently, microdosimetry has been employed in [6] using ideal trapezoidal pulses 3 and 10 ns long, to estimate the pulse amplitudes and waveforms delivered at the single cell level, including cell compartments dispersivity on the basis of accurate cell dielectric descriptions [7], [8].

Nevertheless real pulse generators are not able to deliver ideal waveforms especially when coupled with biological samples, as can be seen in [9]-[11] where a versatile nanosecond pulse generator has been developed. This device, combining microstrip-line technology and laser-triggered photoconductive semiconductor switches (PCSSs), is able to deliver, on a 50 Ω adapted load, monophasic and biphasic pulses 2 ns long with maximum amplitude around 2 kV.

Therefore a comparison among "ideal" and "real" waveforms delivered at the cell membrane is desirable even to optimize the generator performances and its effective utilization.

Hence in this paper, we propose a microdosimetric investigation at a single cell level using as sources both ideal and real (measured and simulated) nsPEF waveforms delivered by the generator in [9] to the 50 Ω matched load.

The first aim of this work is to understand the role of the delivered waveform on TMP and pore density values.

In a first step, the efficiency of monophasic and biphasic ideal pulses was investigated, and then real and ideal waveforms were compared. This is necessary in order to understand the role of both the energy content and of the waveform of the pulse delivered at the microscopic scale. Such study seems useful in the perspective of a more controlled and effective nsPEF biological experimentations devoted both to mechanism comprehension and medical treatment applications.

The paper is organized as follows: in Section II.A of the Material and Methods the TMP calculation is highlighted. While in Sections II. B and C information on simulated

pulses and pore density calculation is reported, respectively. In Results section III.A monophasic and biphasic waveforms is evaluated and their efficiency at the level of cell membrane discussed. Then, in section III. B, simulated and measured real pulses in [9] are compared with ideal trapezoidal signals. Finally, conclusions are given in section IV.

II. Materials and Methods

A. TMP Calculation

The EM field at cell membrane level was calculated on a three-layered spherical cell taking into account the extra cellular medium, the membrane, and the cell cytoplasm.

The dispersive dielectric properties of the membrane were accounted using Debye dispersion as in [6] considering a static permittivity ε_{SM} of 11.7, a high-frequency permittivity $\varepsilon_{\infty M}$ of 4, a relaxation frequency f_{relaxM} of 180 MHz and a ionic conductivity σ_{dcM} of 1.1×10^{-7} S/m. These parameters were obtained using a rigorous theoretical-experimental methodology coupling dielectric measurements of biological solutions with fitting techniques on the basis of mixing formulas [7].

For cytoplasm and extra-cellular medium phosphate buffer saline solution was used with the following Debye parameters: ε_{SPBS}=67, $\varepsilon_{\infty PBS}$=5, $f_{relaxPBS}$=17.9 GHz and σ_{dcPBS}= 0.55 S/m, measured at 27°C [10].

Typical cell dimensions with a radius of 10 μm and a membrane thickness of 10 nm where also used in microdosimetric simulations.

Due to the small cell dimensions (up to 50 μm) with respect to the field wavelength, the microdosimetric problems can be considered as quasi-static ones and solved using the Laplace's equation [12]. To take into account the wide spectral content of nanosecond pulses a suitable algorithm was developed as also extensively described in [6]. A Fourier transform was used to convert the temporal samples of the pulses in frequency domain where Laplace calculation is performed. The cell compartments dispersivity was included within the continuity conditions at the interfaces of the different media. A sampling time of 30 ps and a total observation time of 2.43 μs were carefully chosen to ensure wide spectral resolution and proper time signal reconstruction. Finally inverse Fourier transform of the frequency samples was computed to come back to time domain quantities.

B. Used Pulses

Ideal trapezoidal monophasic and biphasic signals were used, 1.4 ns wide, with rise and fall times equal to 300 ps (see Fig. 1) considering pulse amplitudes of 8.6 MV/m, in agreement with [3].

Real pulses were obtained from [9] and in particular: (i) the SPICE circuital representation of the generator; (ii) the Finite Difference Time Domain (FDTD) full wave simulation, and (iii) the voltage measurements taken across the matched load. The SPICE model is reported in Fig. 2, where the main generator components are shown including the power supply with a bias resistor, two PCSSs, an ideal transmission line (TXD) with propagation delay of 0.7 ns, and an adapted 50 Ω load. Even if such a model is able to predict quite accurately the generated waveform, as noted in [9], it completely disregards strip tapering near the PCSS all line discontinuities as well as radiation losses, that are accounted in the FDTD simulations.

In Fig. 3, the real waveforms voltages, already shown in Fig. 5 of [9], are reported for the biphasic signals. The amplitude of the signals was adapted in order to have the same energy of the ideal pulses.

C. Pore Density Evaluation: Asymptotic Electroporation Model

The density of hydrophilic membrane pores is actually a complicated function monotonically increasing with the TMP.

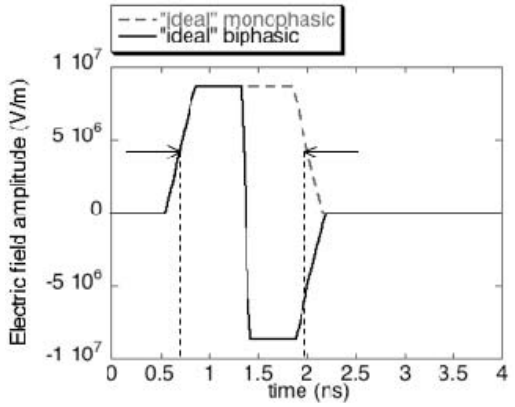

Fig. 1. Ideal monopahsic and biphasic pulses. The instants at which pulse duration is calculated are also reported.

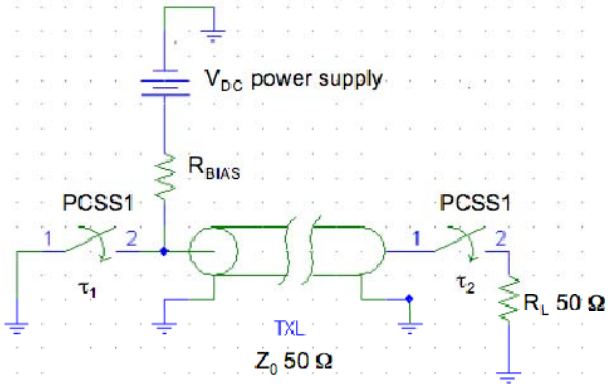

Fig. 2. Circuital representation of the 50 Ω generator terminated on an adapted 50 Ω load.

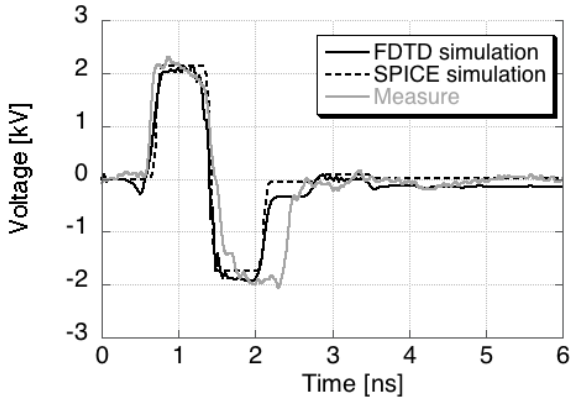

Fig. 3. The voltage of the real pulses across the matched 50 Ω load is reported including SPICE circuital representation of the generator, the FDTD full wave simulation, and the measurement.

However, in the nanosecond time scale, where the pore creation is assumed to dominate over pores enlargement and destruction, the asymptotic electroporation model can be employed as noted in [13].

The authors adopted this model in [6] and in this paper. Pore density indicates the number of pores per unitary membrane area and usually is comprised between two limiting values: the first equal to 10^{15} m^{-2} is known as poration threshold (PT) and the other of 10^{18} m^{-2} is indicated as feasibility threshold (FT). The PT value is typically sufficient to cause a reversible membrane breakdown while the FT is the maximum feasible pore density implying that 1 nm^2 of the membrane is completely porated [6]. Further, poration time defined as the time interval needed to reach the PT is calculated. Even if this asymptotic description is based on empirical parameters, it is the model mostly used for nanoporation quantification.

III. Results

A. Comparing monophasic and biphasic ideal pulses

All the data shown in the following are taken at the cell pole, where the electric field is maximum.

TMP induced by both monophasic and biphasic pulses sharply increases passing the TMP threshold of 1 V required to start the poration phenomenon, however biphasic pulse induced the highest TMP peak value (data not shown).

The time-frequency representation (spectrogram) of the electric field amplitude calculated within the cell membrane is reported in Fig. 4 for both the pulses. High frequency components are prevalent in the spectrogram obtained using the biphasic pulse (Fig. 4.b). Such prevalence of high frequencies implies lower values of the membrane permittivity with a consequent increase of the electric field in the membrane. Therefore, a higher pore density plateau value of 7×10^{17} m^{-2}, which determines an almost complete membrane poration, is achieved with respect to the monophasic pulse where a pore density of 1.5×10^{13} m^{-2}, under the PT, is attained (data not shown).

B. Comparing "real" and "ideal" trapezoidal pulses

Since the previous analysis highlights the higher effectiveness of the biphasic pulses, they are used in real and ideal waveforms comparison. TMP time courses obtained with the biphasic real pulses (solid, dashed gray lines and dashed black line) and the ideal one (solid black line) are reported in Fig. 5. Comparable TMP peaks are achieved for all signals during the positive phase.

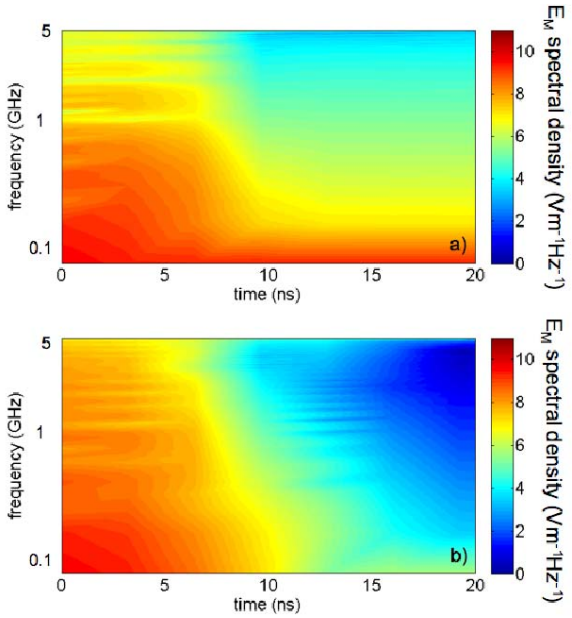

Fig. 4. a) The time-frequency representation (spectrogram) of the electric field amplitude within cell membrane is reported for the monophasic ideal pulse. b) spectrogram of the electric field amplitude within cell membrane for the biphasic ideal pulse.

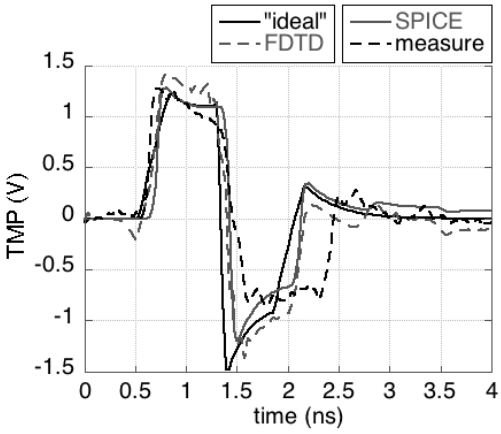

Fig. 5. TMP time courses obtained with the biphasic ideal and real pulses including SPICE circuital representation, FDTD full wave simulation, and measurement.

TABLE I
PORE DENSITY PLATEAU AND PORATION TIME

	Pore density (m^{-2})	Poration Time (ns)
ideal	7.0×10^{17}	0.78
FDTD	1.7×10^{16}	1.3
SPICE	1.0×10^{13}	-
Measure	8.8×10^{12}	-

On the contrary, during the negative phase, the TMP induced by the ideal pulse has a more negative peak due to the sharper decrease of the delivered waveform (see Fig. 3). This phase transition becomes longer in real signals due to the transmission delay along the stripline of the generator. Moreover, FDTD simulations ad measurements account also for losses due to radiation, mismatching of the line tapering near the PCSS, and other line discontinuities. As a consequence, the ideal signal induces a higher pore density in the membrane, as reported in Table I. In the same table, pore densities for real signals are also reported. Looking at these results, it is evident that, while the ideal signal is effective in porating the membrane, the real ones induce poration values always under the plateau reached by the ideal signal. Indeed, in one case (FDTD pulse) the induced pore density plateau is slightly above the PT and in the others (measure and SPICE) it is even under such a threshold (see Table I). Moreover, different poration times (Table I) are reported for ideal and real (FDTD) signals, indicating that also this parameter is strongly variable in dependence on the pulses waveform characteristics.

IV. CONCLUSIONS

A microdosimetric analysis using ideal and real pulses was carried out in this paper. To perform this goal, a recently developed algorithm for nsPEF based on Laplace equation and able to take into account cell compartment dispersivity was employed [6]. Pore density distribution was then calculated using the asymptotic electroporation model [12].

As first result, the poration efficiencies induced by ideal trapezoidal 1.4 ns long monophasic and biphasic pulses were tested. Biphasic pulse resulted in higher poration efficiency due to the prevalence of the high frequency spectral components. Indeed, at such frequencies (>100 MHz) the dielectric relaxation of the membrane occurs leading to a permittivity reduction. Consequently, the low membrane permittivity determines an increase in electric membrane field and TMP then enhancing pore density values.

Successively, a comparison between biphasic real and ideal waveforms was carried out. The ideal pulse induced the lowest TMP peak values during the negative phase of the curve leading to the highest pore density plateau value of $7\times10^{17}\ m^{-2}$. On the contrary real waveforms including different loss effects as the line-tapering mismatch or radiation are still not able to reach the PT. This result has a direct incidence during the steps of the design and realization of a new generator, evidencing that a detailed optimization of the device has a fundamental impact on the performances of the pulses delivered at the single cell level. Moreover this point seems even more critical when the generator is connected to a biological load presenting frequency variable impedance within the pulse bandwidth [7]. In that case a wide band matching with the load is of mandatory importance for effectively inject defined pulses on cells. This represents the essential requirement for highly controlled bio-experiments needed for the investigation of nsPEF action mechanisms and the development of medical treatments.

REFERENCES

[1] R. P. Joshi, K. H. Schoenbach "Biolectric effects of intense ultrashort pulses" *Critical Review in Biomed. Eng.*,vol. 38, no. 3, pp. 255–304, 2010.

[2] P. T. Vernier, M. J. Ziegler, Y. Sun, M. A. Gundersen, and D. P. Tieleman, " Nanopore-facilitated voltage driven phosphatidilserine translocation in lipid bilayer-in cell and in silico" *Biophys.*, vol. 3, pp. 233–247, 2006.

[3] G. L. Craviso, S. Choe, P. Chatterjee, I. Chatterjee, P. T. Vernier, "Nanosecond electric pulses: a novel stimulus for triggering Ca^{2+} influx into chromaffin cell via voltage-gated Ca^{2+} channels", *Cell Mol. Neurobiol.*, vol. 30, pp. 1259-1265, 2010.

[4] U. Pliquett, R. P. Joshi, V. Sridhara, and K. H. Schoenbach, "High electrical field effects on cell membranes", *Bioelectrochem*., vol. 70, pp. 275-282, 2007.

[5] L. Chen, A. L. Garner, G. Chen, Y. Jing, Y. Deng, R. J. Swanson, J. F. Kolb, S. J. Beebe, R. P. Joshi, K. H. Schoenbach, "Nanosecond electric pulses penetrate the nucleous and enhance speckle formation", *Biochem. Biophys. Res. Com.,* vol. 364, pp. 220-225, 2007.

[6] C. Merla, A. Paffi, F. Apollonio, P. Leveque, G. d'Inzeo, and M. Liberti, "Microdosimetry for nanosecond pulsed electric field applications: a parametric study for a single cell", IEEE Trans. Biomed. Eng., accepted, early access on line.

[7] C. Merla, M. Liberti, F. Apollonio, G. d'Inzeo, "Quantitative assessment for dielectric parameters of membrane lipid bi-layers form RF permittivity measurements", *Bioelectromagnetics*, vol. 30, pp. 286-298, 2009.

[8] C. Merla, M. Liberti, F. Apollonio, C. Nervi, G. d'Inzeo, "A 3D microdosimetric study on blood cells: a permittivity model of cell membrane and stochastic electromagnetic analysis*", IEEE Trans. Microwave Theory Tech*., vol 58, no. 3, pp.691-698, 2010.

[9] C. Merla, S. El-Amari, F. Danei, M. Liberti, F. Apollonio, D. Arnaud-Cormos, V. Couderc, and P. Leveque, "Microstrip-based nanosecond pulse generator: numerical and circuital modeling", *in Proc. IEEE-MTT-S Int. Microw. Symp. (IMS' 2010),* Anaheim, CA, pp. 101-104.

[10] C. Merla, S. El-Amari, M. Kenaan, M. Liberti, F. Apollonio, D. Arnaud-Cormos, V. Couderc, P. Leveque, "A 10 ohm high voltage nanosecond pulse generator", *IEEE Trans. Microwave Theory Tech.*, vol. 58, no. 12, pp. 4079–4085, 2010.

[11] S. El-Amari, M. Kenaan, C. Merla, B. Vergne, D.Arnaud-Cormos, P. Leveque and V. Couderc, "Kilovolt, nanosecond and picosecond electric pulse shaping by using optoelectronic switching", *IEEE Photon. Technol. Lett.,* vol. 22, no. 21, pp. 1577-1579, 2010.

[12] J. Stratton, *Electromagnetic Theory*. New York: McGraw Hill, 1941.

[13] K. C. Smith, T. Gowrishankar, A. Esser, D. Stewart, and J. C. Weaver, " The spatially distributed dynamic transmembrane voltage of cells and organelles due to 10-ns pulses: meshed transport networks", *IEEE Trans. Plasma Sci.,* vol. 34, no. 4, pp. 1394-1404, 2006.